Computational Mechanics 26 (2000) 129–139 © Springer-Verlag 2000

Evolutionary topology and shape design for general physical field problems

G. P. Steven, Q. Li, Y. M. Xie

Abstract As a practical tool for design engineers, evolutionary techniques for structural topology, shape and size optimisation have successfully resolved the whole range of structural problems from frames to 2D and 3D continuums with design criteria of stress, stiffness, frequency and buckling. In view of the generality of the finite element formulation using either a variational calculus or weighted residual approach, it is logical to extend its applications to other steady state field problems in mathematical physics governed by partial differential equations. The range of physical problems falling to this category includes heat conduction, incompressible fluid flow, elastic torsion, electrostatics and magnetostatics, etc. This paper discusses the general principles involved in setting up the adaptive evolutionary algorithms that have finite element techniques as the analysis engines. To avoid the complexity of classical solutions, the proposed method develops a simple outer loop procedure consisting of finite element analysis and design modifications. Illustrative examples are presented to demonstrate the capability in solving the above-mentioned physical field situations.

1 Introduction

The advent of computational methods for field problems in physics has given the analyst the ability to solve almost any problem that can be posed. In engineering the purpose of such calculations has generally focused on solving the physical problem to find spatial and temporal values of the field variable, such as temperature, shear stress, velocity, voltage, etc. There are often over-arching design criteria that an analyst can examine to ensure that the design complies with the specifications. For example, in structural mechanics strength and stiffness are examined to avoid excessive distortions or stresses, in heat flow temperature is examined to avoid melting and so on. Traditionally, this process is regarded as a direct problem.

On the other hand, a designer often needs to consider whether the topology or shape of the designed field is optimum or, more realistically, as good as possible. The definition of an optimum may vary from one situation to the another according to the environments the structure has to live in and what is expected of it. Nevertheless the concept is related to an inverse problem whereby one poses the result and asks for the problem definition.

It is well known that the direct steady state field problems governed by partial differential equations have received wide attention since the last century. In this category, finite element techniques have become one of most prevalent and useful numerical tools in the last three decades (refer to Hinton and Owen, 1979). However, physical field shape or topology optimizations, as one of the most typical inverse problems, have achieved far less popularity than the direct problem for following two reasons (Neittaanmaki et al., 1996). Firstly, in many practical situations, the complexity of the field problem itself, leads to difficulties in accommodating an optimal approach. Secondly, traditional structural optimization methods usually require a great deal of gradient information to achieve a solution (Haftka, 1981; Lee, 1993; Park and Yoo, 1988; Saigal and Chandra, 1991). This in turn needs the appropriate choice of design variables and many finite element solutions to determine these gradients in a semi-analytic way generally using finite differences.

To overcome the difficulties mentioned above, Evolutionary Structural Optimization (ESO) algorithms are employed to deal with the optimization of the steady field problems in this paper. Previous investigations on this technique have demonstrated the successful applications for various structural problems since 1993 (Xie and Steven, 1993). It has been recognized that the most significant advantages of this method are its simplicity in physical concept and easiness in computer implementation (Xie and Steven, 1997). We consider the method has sufficient generality and can resolve some of field optimizations in a simple and easy manner. The paper has the purpose of developing a systematic methodology for the steady field design problems.

G. P. Steven (✉), Q. Li
Department of Aeronautical Engineering,
The University of Sydney,
NSW 2006, Australia

Y. M. Xie
School of The Built Environment,
Victoria University of Technology,
P. O. Box 14428, Melbourne City Mail Centre,
VIC 8001, Australia

The research is funded by the Australian Research Council. During the study, the second author has been awarded the Australian Postgraduate Award and an Aeronautical Engineering Scholarship at The University of Sydney.

2
Optimality criteria for steady state field problems

Mathematically, the steady-state behaviour of many physical phenomena can be described by a quasi-harmonic equation

$$\frac{\partial}{\partial x}\left(K_x\frac{\partial \phi}{\partial x}\right)+\frac{\partial}{\partial y}\left(K_y\frac{\partial \phi}{\partial y}\right)+\frac{\partial}{\partial z}\left(K_z\frac{\partial \phi}{\partial z}\right)+Q=0 \ , \tag{1}$$

subject to, either the Dirichlet boundary condition,

$$\phi=\phi_d \ , \tag{2}$$

or the Cauchy boundary condition

$$K_x\frac{\partial \phi}{\partial x}\ell_x+K_y\frac{\partial \phi}{\partial y}\ell_y+K_z\frac{\partial \phi}{\partial z}\ell_z+g+\kappa(\phi-\phi_a)=0 \ , \tag{3}$$

at any boundary point, where ϕ is the unknown function of field variable, K_x, K_y, K_z represent known parameters associated with the physical properties of the domain, Q denotes the source or excitation function, g, κ and ϕ_d are known a priori and ℓ_x, ℓ_y, ℓ_z stands for direction cosines of the outward normal to surface. Equations (1)–(3) comprises a well-posed elliptic boundary value problem, whose solution by finite element method can be found via a classical variational principle (Hinton and Owen, 1979).

Field optimization aims at achieving the best physical performance by appropriately distributing (re-distributing) the material. From the standpoint of finite element discretization, alteration of material allocation can be simply represented by varying elemental presence (material property = type 1 or higher) or absence (material property = type 0). That is to say that the element itself, rather than any associated parameter such as nodal coordinate or element density, is treated as the design variable herein. For this reason, it is essential to assess the relative performance of every element in order to achieve an optimization.

In view of the common characteristics of different physical categories, two main points need to be taken into account in determining the elemental optimality criteria. Firstly, the finite element formulations of various field phenomena are analogous, regardless of physical meaning. That is to say, the same finite element solver for a specific physical issue can also be employed for other problems without making any major modification. This economically extends the application ranges of existing finite element solvers. Hence, it would be beneficial to unify the formulations of optimality criteria for various field problems. Secondly, although designers may proficiently use finite element packages, they usually have no access to the source codes. For this reason, it would be favorable to develop optimality criteria only on the basis of the standard inputs and outputs of any finite element program. In other words, the finite element package is better to be viewed as a 'black box' in the entire design optimization loop.

2.1
Heat conduction problems

In steady-state heat conduction, parameters K_x, K_y, K_z represent thermal conductivities, variable $\phi(x,y,z)=T$ denotes the temperature distribution of the analysis domain, and Q stands for internal heat generation. From this, heat flux is subsequently calculated as $\mathbf{F}=-\mathbf{K}\cdot\nabla\phi$.

In a fully fluxed or iso-fluxed design, all elements in the design domain are expected to carry as uniform a heat quantity as possible. To identify the heat transfer ratio of an element of the material, a heat flux density is defined as (Li et al., 1997, 1999b)

$$J^{\mathrm{e}}=\frac{1}{V_{\mathrm{e}}}\int_{V_{\mathrm{e}}}\|\mathbf{F}\|_2\,\mathrm{d}V_{\mathrm{e}} \ , \tag{4}$$

where V_{e} denotes the volume of the element, and $\|\mathbf{F}\|_2$ stands for the second norm, i.e. the root of mean square of the flux vector. In a typical heat transfer region, it is common that flux levels in some elements are quite lower than those in others. This means that elements contribute differently to the heat conduction functionality of the solution domain. To estimate the relative efficiency of each element to conduct heat, a dimensionless factor is computed as

$$\alpha^{\mathrm{e}}=J^{\mathrm{e}}/J^{\max} \ , \tag{5}$$

where $J^{\max}$ represents the highest flux density in entire heat field.

2.2
Elastic torsion problems

For pure torsion of a prismatic bar, the cross section of which is the solution domain, the parameters K_x, K_y stand for the reciprocal of shear moduli ($K_z=0$ in this case), variable $\phi(x,y)$ denotes the Prandtl stress function, and Q represents twice the rate of twist. The elemental shear stress components can be subsequently calculated as $\tau_{xz}=\partial\phi/\partial y$ and $\tau_{yz}=-\partial\phi/\partial x$. The torsion field always satisfies Dirichlet-type boundary conditions as

$$\begin{cases}\phi=0, & (x,y)\in\Gamma_{\mathrm{o}}\\ \phi=C_i, & (x,y)\in\Gamma_{\mathrm{i}}\end{cases} \ , \tag{6}$$

where Γ_{o} and Γ_{i} stand for the exterior and interior boundaries respectively (Adali, 1981; Li et al., 1999a).

In the traditional solutions, the optimal problems are constructed either to minimize the cross-sectional area subject to a prescribed torsional rigidity constraint or to maximize the rigidity subject to a given area (Polya, 1948; Adali, 1981). Obviously, such optimizations mainly reflect a stiffness requirement of the designs, where the material is properly allocated to ensure a stiffest design. On other circumstances, the designer may wish to seek an iso-strength criterion, e.g., to find an evenly or fully stressed design. For this purpose, an appropriate reference criterion related to material stress level is needed. One of most frequently used measures of the material shear strength can be the resultant of the shear stress components, defined as (Hinton and Owen, 1979).

$$\tau = \sqrt{\tau_{xz}^2 + \tau_{yz}^2} = \sqrt{\left(\frac{\partial \phi}{\partial y}\right)^2 + \left(-\frac{\partial \phi}{\partial x}\right)^2} \quad . \tag{7}$$

As a result, the resultant shear stress level is adopted to estimate the efficiency of material usage in the sense of shear strength. Like other elastic structural mechanics problems, it often happens that the stress levels of some elements are lower than others in the solution domain. To measure the relative efficiency of elemental material usage, a dimensionless factor is calculated with respect to the highest shear stress level as

$$\alpha^e = \tau^e / \tau^{max} \quad . \tag{8}$$

A larger or a smaller elemental resultant stress indicates a higher or a lower material usage efficiency respectively.

A special feature of the torsion problem in multiply connected regions is the treatment of the Dirichlet-type boundary conditions, in which the stress function on an exterior boundary is always set to zero while on any interior boundary there needs to be some different constants. To avoid the difficulties in determining the internal boundary constants, a soft kill and restore technique is introduced in the ESO algorithm whereby, removing internal elements is represented by assigning a very low shear modulus rather than creating a genuine inner boundary in a mathematical sense (Hinton and Owen, 1979; Li et al., 1999a).

2.3
Incompressible fluid flow problems

In an inviscid, incompressible irrotational flow, parameters K_x, K_y, K_z equals to a unity amount, field variable $\phi(x, y, z)$ represents stream function or potential function, and $Q = 0$. Once the field variable $\phi(x, y, z)$ is solved from Eq. (1), fluid velocity is further computed as $\mathbf{V} = \nabla\phi$.

The flow field design usually requires the attainment of a uniform flow velocity (Madsen, 1995). To assess the role that an element plays in the flow field, a velocity density is calculated as

$$J^e = \frac{1}{V_e} \int_{V_e} \|\mathbf{V}\|_2 \, dV_e \quad . \tag{9}$$

Furthermore, the relative velocities between elements is estimated as

$$\alpha^e = J^e / J^{max} \quad , \tag{10}$$

by which the relative efficiency level of elemental material usage is indicated. A lower velocity level reflects the flow over such elements cannot work with a full speed, in other words, the elemental material or field space is not efficiently utilized.

2.4
Electrostatic problems

In an electrostatic field, parameters K_x, K_y, K_z represent permittivity, field variable $\phi(x, y, z)$ denotes the electric potential of the analysis domain, and Q stands for charge density. The electric field intensity can be further computed from $\mathbf{E} = -\nabla\phi$.

Under many circumstances, the design of an electric field is expected to have the distribution of the field intensity as uniform or even as possible (Neittaanmaki et al., 1996). To indicate the field intensity level at unity volume, an electric field intensity is computed as

$$J^e = \frac{1}{V_e} \int_{V_e} \|\mathbf{E}\|_2 \, dV_e \quad . \tag{11}$$

Also, it is often the case that different finite elements have quite different field intensities. To assess the relative efficiency of a field element, a dimensionless factor is calculated as

$$\alpha^e = J^e / J^{max} \quad . \tag{12}$$

Higher efficiency factors reflect that the corresponding elements play a more important role than those with lower efficiency factors.

2.5
Magnetostatic problems

In a magnetostatic field, parameters K_x, K_y, K_z are reluctivity, field variable $\phi(x, y, z)$ denotes the magnetic potential of analyzed domain, and Q stands for charge density or forward current. The magnetic flux level is subsequently computed from $\mathbf{B} = \nabla \times \phi$ (Jin, 1993).

In this category, one of the most often faced design criteria is to seek a uniform or even magnetic field density for a given design domain (Neittaanmaki et al., 1996). Similarly to the other field problems as discussed above, a magnetic flux density is introduced to indicate the performance of a field element as

$$J^e = \frac{1}{V_e} \int_{V_e} \|\mathbf{B}\|_2 \, dV_e \quad . \tag{13}$$

Likewise, the relative efficiency of magnetic field element is also evaluated as

$$\alpha^e = J^e / J^{max} \quad . \tag{14}$$

3
Generalised evolutionary optimisation procedures

It has been acknowledged that engineers often design from a more conservative situation to a less conservative one as confidence increases. For this reason, the classical ESO process starts from a large or an over-designed initial design space, and then gradually removes redundant or inefficient material. Under other circumstances, the designers may also modify an initial design through more logical distribution of the same amount of material. For these two outcomes, the ESO approach to the field optimization is developed into two different procedures as follows.

3.1
Procedure for the volume reduction

Typically, after finite element analysis, the efficiency levels of some elements are quite lower than others. From the viewpoint of equal efficiency, it is logical that such less efficiently utilized material is gradually removed from the solution domain. In the ESO method, the criterion of element removal is determined by a threshold efficiency level as

$$\alpha^e \leq RR_{SS} \ , \tag{15}$$

where, borrowing from its origins in structural optimization, RR_{SS} is still called Rejection Ratio or threshold efficiency level. The process of the element removal is repeated using the same value of RR_{SS} until an ESO Steady State (SS) is reached, which means that there are no more elements that can be removed at the current iteration. At this stage an Evolutionary Rate (ER) is introduced so that

$$RR_{SS+1} = RR_{SS} + ER \ . \tag{16}$$

A typical value for ER is around 1% to ensure a smooth change between two steady states. With the increased rejection ratio or threshold efficiency, the cycle of finite element analysis and element removal takes place again until a new steady state is reached. The evolution rate is set to increase the threshold efficiency to a higher level, whereby the usage efficiency of the remaining material becomes more uniform than before.

To generalize the procedures, a soft kill technique (Mattheck, 1998; Hinton and Sienz, 1995) is adopted herein, where any internal hole is assumed to compose of a material with relatively low material property (say $10^{-3} \sim 10^{-6}$ of those of the solid material). In the computation, the degraded property elements have a negligible contribution to the physical capacity, and are therefore regarded as voids in the structure. Theoretically, this makes the region remain singly connected, in which case, the interior boundary conditions are automatically adaptive. In practice, the treatment is easily implemented via only assigning the property value of the candidate elements to a prescribed low value.

For clarification, the ESO procedure for the generalized field problems subject to volume reduction is briefly described as follows:

Step 1: Discretize the design and non-design domains using a dense FE mesh, define ESO driving parameter ER and RR_0;
Step 2: Carry out FEA to solve the field problem as governed by Eqs. (1)–(3);
Step 3: Assign the material property of candidate elements to a prescribed low value if their relative efficiency levels satisfy Eq. (15);
Step 4: If an ESO steady state is reached, increase RR_{SS} by ER as Eq. (16) and set $SS = SS + 1$, repeat Step 3; Otherwise, repeat Steps 2 to 3 until an optimum is attained.

3.2 Procedure for the constant volume

In the previous procedure, the optimization process is carried out by progressively removing least efficient material from the structure. Therefore, the total solid area/volume of the physical domain is gradually reduced during the evolutionary process. Sometimes, however, a designer may wish to improve the performance of a physical field while keeping its weight (or volume or cross-section area) constant. This can be achieved by progressively shifting material from the ‘strongest’ location to the ‘weakest’ location in a volume conserving manner. Through such a process, the lowly efficient (under-utilized) material becomes more efficient (over-utilized) than before until an evenly utilized allocation of material is attained.

To implement the procedure, an appropriate initial shape is modeled, where the solid and void regions can usually be represented by a relatively high and a relatively low material properties respectively. In terms of the relative efficiency levels, a small number of under-utilized elements are removed from the solid regions by simply switching their material property to the void one. Meanwhile, the same number of void elements, adjacent to the solid elements with the highest efficiency, is switched to the solid property. As a result, this process maintains the number of solid elements unchanged at each iteration.

For clarification, the ESO procedure for generalized field problems subject to the constant volume/cross-sectional area is briefly described as follows:

Step 1: Discretize the design and non-design domains using a dense FE mesh, the initial solid and void regions are represented by high or low material properties respectively, and define ESO driving parameter ER and RR_0;
Step 2: Carry out a FEA to solve the field variable problem as governed by Eqs. (1)–(3);
Step 3: Switch the material property of candidate solid elements onto the void one if their relative efficiency levels satisfy Eq. (15), and then change the same number of void elements adjacent to the highest efficiency elements onto solid ones;
Step 4: If an ESO steady state is reached, increase RR_{SS} by ER as Eq. (16) and set $SS = SS + 1$, repeat Step 3; Otherwise, repeat Steps 2 to 3 until an optimum is attained.

4 Illustrative examples

The following examples are used to demonstrate the capabilities of the proposed ESO procedure in solving shape and topology optimization for several typical steady state field problems, in which these two procedures, volume reduction or conservation, are alternatively applied. For simplicity, all examples are modeled using two-dimensional regular four node quadrilateral elements. In all the optimization processes, an initial rejection ration of $RR_0 = 0$ and an evolution rate of $ER = 1\%$ are set up. In the evolution history pictures shown below, the black areas represent the remaining solid elements and the small dots represent the nodes of the initial finite element model.

4.1 Heat conduction design

4.1.1 Shape design example, constant volume

As the first design case, a field with three heat flux inputs is considered as illustrated in Fig. 1a, in which the design

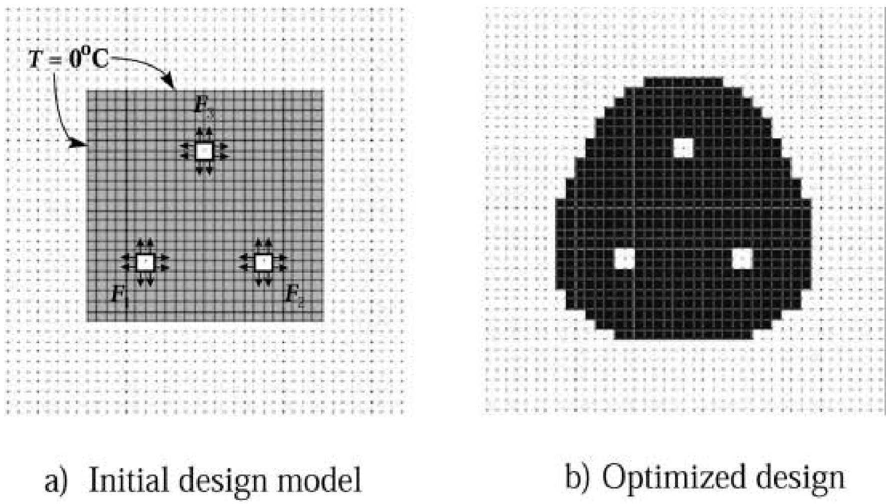

Fig. 1a, b. Heat flow shape design of the exterior boundary, subject to the constant volume. **a** Initial design model. **b** Optimized design

domain is discretized by a finite element mesh of 40×40 elements. Initially, a square area with 24×24 elements is considered as the conduction design as Fig. 1a. The optimization is carried out through a material preservative manner. The temperature at the outer boundary of the conduction solid is always maintained at 0 °C, regardless of position.

Figure 1b displays the optimum design, where the boundary material has been gradually shifted from the under-designed area to the over-designed area. Figure 2 shows the evolution histories of the flux densities. It is clear that, with the evolution process, the flux deviation between the highest and the lowest becomes smaller and smaller until a constant situation is reached at around iteration 25. This reflects the heat flux densities of boundary elements become as evenly distributed as possible, i.e. iso-fluxed. Theoretically, such deviation between the maximum and the minimum should be close to zero for an absolutely iso-fluxed shape. However, for a fixed grid approach like the ESO, it is rarely possible to obtain such a perfect iso-fluxed profile due to the approximation of the smooth boundary by a jagged profile and the imposition of the non-smooth Dirichlet thermal boundary. Consequently, a constant deviation has indicated a stable state for the shaped profiles.

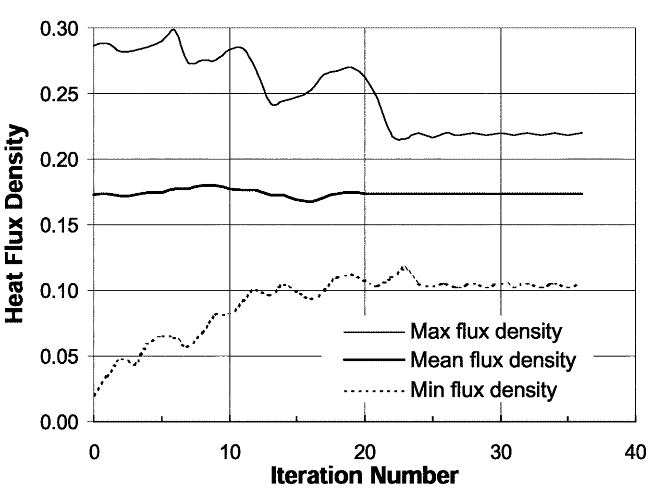

Fig. 2. Evolution histories of heat flux densities of boundary elements

4.1.2
Topology design example, volume reduction

To show the topology optimization capabilities of the ESO for field problems, a printed circuit board (PCB) substrate subjected to steady heat conduction is considered. Apart from the obvious provision of a base for the electrical circuitry, the main functional demand on a PCB substrate is to dissipate the highest amount of thermal energy with a limited amount of material. In accordance with the criterion of optimizing thermal performance, the elements with a relatively low flux level are gradually eliminated from the design domain. As a result, a design topology with more uniform flux density or a smaller flux variation is achieved. In other words, the thermal efficiency or conduction performance of the heat field becomes more and more uniform.

In a second design case, the design space (meshed in 53×33 elements) consists of design and non-design domains as shown in Fig. 3a. Four steady heat flux loading, F_1, F_2, F_3 and F_4, are set to 10 kW/m^2, which are generated from several major electronic components mounted on the PCB. The temperature on the outer boundary are maintained at 0 °C throughout the evolution process. Figure 3b shows the optimized topology subjected to a volume ratio (the ratio of current volume to the initial volume) of $V/V_0 = 70\%$.

This case we have just examined had the four heat sources operating at the same time. In reality it may be the case that those differently located electronic components work at different times. Obviously the separate effects of the individual heat sources on the field are quite different from the simultaneous operation of all heat sources. To deal with such multiple heat load cases, a weighted average scheme is employed to estimate the overall usage efficiency of an element as

$$\alpha^e = \sum_{i=1}^{LCN} w_i \alpha_i^e \ , \tag{17}$$

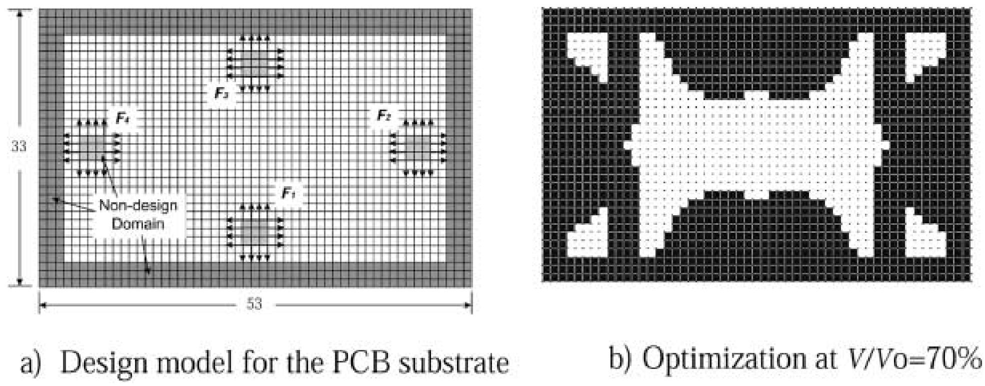

Fig. 3a, b. Heat flux based topology design for the PCB substrate. **a** Design model for the PCB substrate. **b** Optimization at $V/V_0 = 70\%$

where LCN is the number of heat load cases, α_i^e represents the elemental efficiency factor for the ith heat case, and w_i denotes the weighting coefficients for the ith heat case. In this scheme, the weighting coefficient w_i provides a means to treat the multiple heat sources differently. Figure 4a gives a design with the equal weights of $w_1 = w_2 = w_3 = w_4 = 0.25$, which may represent all four heat sources having equal operational frequency. To accommodate possible different operation frequencies of various heat sources, uneven weights could be set. Figure 4b corresponds to a design with $w_1 = w_3 = 0.20$ and $w_2 = w_4 = 0.30$. Comparing Fig. 4a with Fig. 4b, it can be seen that when the heat sources 2 and 4 are allocated a higher weight, more material is distributed in the vicinity of these two source regions than before.

4.2 Cross section design for elastic torsional shafts

4.2.1 Design with volume reduction

As the first illustration of a torsion field optimization, the elements are allowed to be removed from both the exterior boundary and the internal region, which may result in a multiply-connected design. A rectangular design domain, meshed with 30×40 elements, is initially generated as Fig. 5a, while Fig. 5b shows the optimized design at volume ratio of 60%. It is interesting to notice that the result based on the fully stressed criterion is in excellent agreement with the most rigid design by Schramm and Pilkey (1993) as shown in Fig. 5c. This indicates that a fully stressed design and a most rigid design share the same optimum profile. This provides further evidence that the fully stressed design criterion is equivalent to the stiffness design criterion (Li et al., 1999c).

Figure 6a plots the evolution histories of the shear stresses. It can be seen that, as more and more inefficient material is removed from the structure, the deviation between the maximum and the minimum stresses becomes smaller and smaller. At a certain stage (around $V/V_0 = 60\%$), both the maximum and the minimum stresses vary at an approximately constant ratio. This reflects a stable state where the stresses on the design boundaries become almost uniform. To monitor the torsional rigidity reduction during material removal, an evolution history of rigidity-volume ratio is plotted as Fig. 6b. At around $V/V_0 = 60\%$, the ratio reaches the extreme. From a rigidity point of view this is also regarded as a result having the best material usage, which corresponds to the topology with an equal wall thickness as shown in Fig. 5b.

4.2.2 Design with constant volume

The design task is to discover, using ESO with a constant cross sectional area, what shape has a most uniform stress distribution. As illustrated in Fig. 7a, a singly-connected solid square bar (meshed by 28×28 elements) is considered as the initial design. In the design process, since the shorter the distance of an element to the section centroid, the lower its shear stress level, this leads to more and more solid elements migrating from interior the

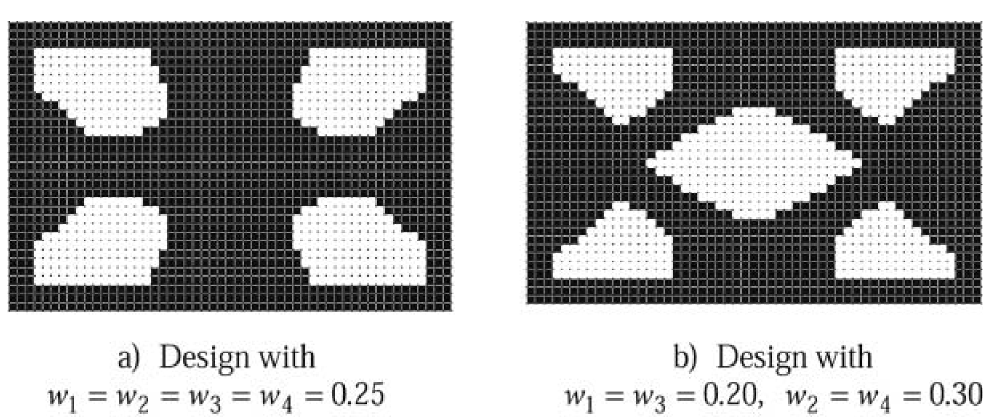

Fig. 4a, b. Topology design for multiple heat load cases ($V/V_0 = 70\%$). **a** Design with $w_1 = w_2 = w_3 = w_4 = 0.25$. **b** Design with $w_1 = w_3 = 0.20$, $w_2 = w_4 = 0.30$

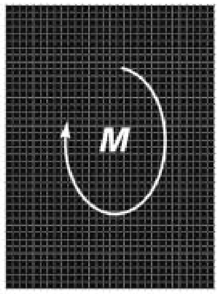

a) Initial design model

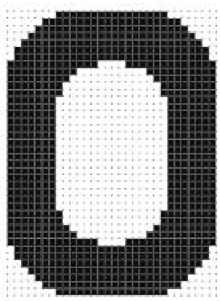

b) Optimized multiply-connected design (V/Vo=60%)

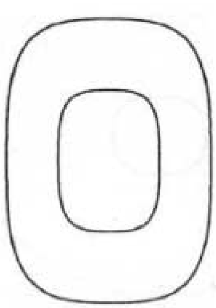

c) Optimized shape by Schramm and Pilkey (1993)

Fig. 5a–c. Optimized design for torsion with volume reduction. **a** Initial design model. **b** Optimized multiply-connected design ($V/V_0 = 60\%$). **c** Optimized shape by Schramm and Pilkey (1993)

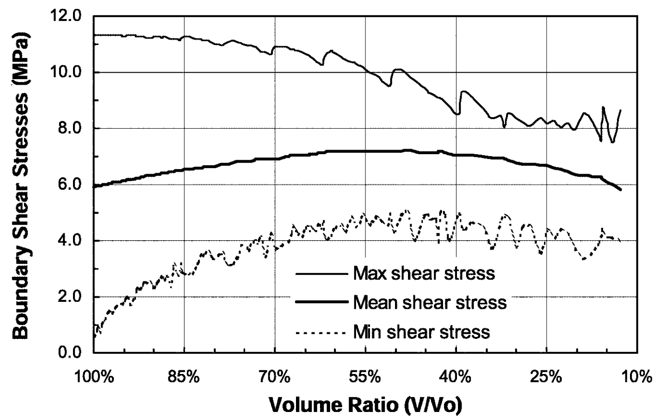

a) Evolution history of the boundary shear stresses

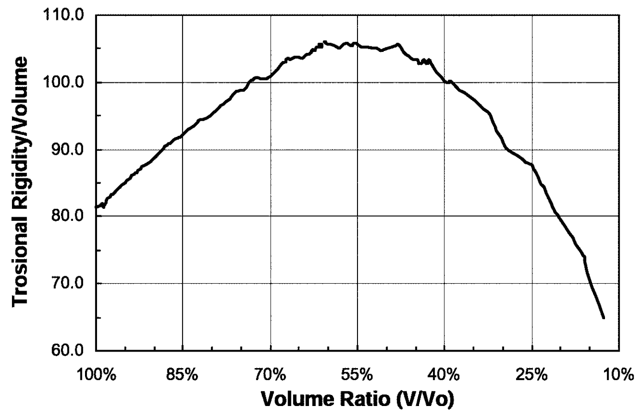

b) Evolution history of torsional rigidity *vs* volume

Fig. 6a, b. Torsional ESO evolution histories with cross-sectional area reduction. **a** Evolution history of the boundary shear stresses. **b** Evolution history of torsional rigidity vs. volume

region to the exterior region. As a result, a circular hole is gradually created at the central area while the straight edges of the exterior profile are progressively rounded. Eventually, the ring shown in Fig. 7b becomes, as expected, the optimized design. From the viewpoint of rigidity, Polya and Weinsten (1950) showed that in the cases of multiply connected cross-sections, a ring bounded by two concentric circles has the highest torsional stiffness. This implies that the optimization of strength and rigidity can be achieved simultaneously. In other words, a ring has both the most uniform stress distribution and the highest torsional stiffness for any possible multiply connected cross-section.

To provide further evidence for the inference, an anisotropic material with $G_x = 2G_y$ is introduced into this case. It is found that the material shift process results in an elliptic annulus with a variable wall thickness as shown in Fig. 8. Again in this case, the evolution history plots, as Fig. 9, give an indication that the reduction in the shear stress deviations and the increase in the torsional rigidity are achieved concurrently. This is also in excellent agreement with the proof by Adali (1981).

4.3
Design of inviscid incompressible flow field

The design example for fluid flow considered herein is a 90° bend. Traditionally such a bend would simple have a quarter of a circular ring shape. The question is, does this produce the most uniform velocity field. Figure 10a illustrates the design model where an inward flow velocity and of 1.0 m/s is input and an equal outwards velocity is output. All other boundaries are non-transmitting and are therefore streamlines. The potential function on interior and exterior boundaries are imposed as 10 and 0 as shown in Fig. 10a.

The evolution process starts from the fully populated domain as Fig. 10a. As the under-utilized elements that are

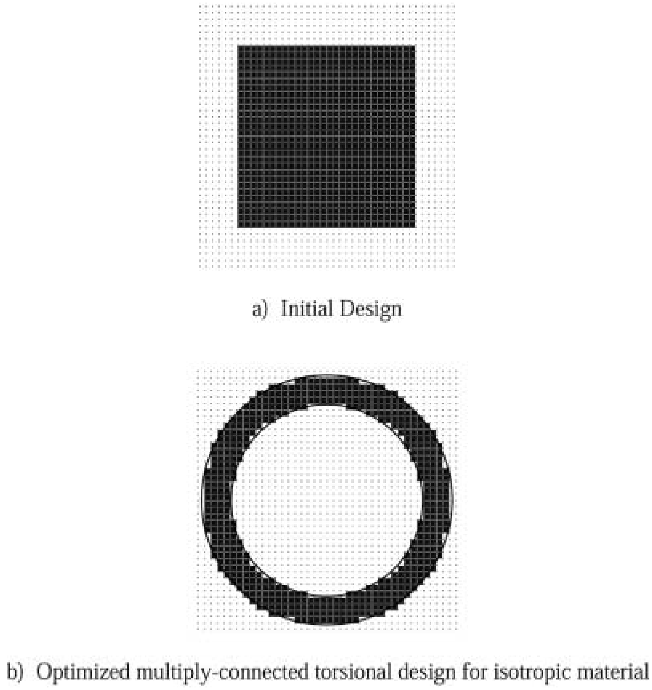

Fig. 7a, b. Optimal exterior and interior boundary torsional design subject to constant volume. **a** Initial design. **b** Optimized multiply-connected design for isotropic material

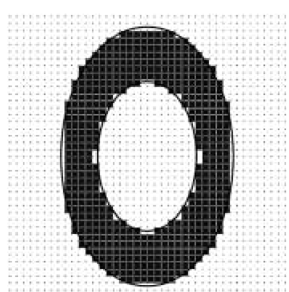

Fig. 8. Optimized multiply-connected torsional design for anisotropic material ($G_x = 2G_y$)

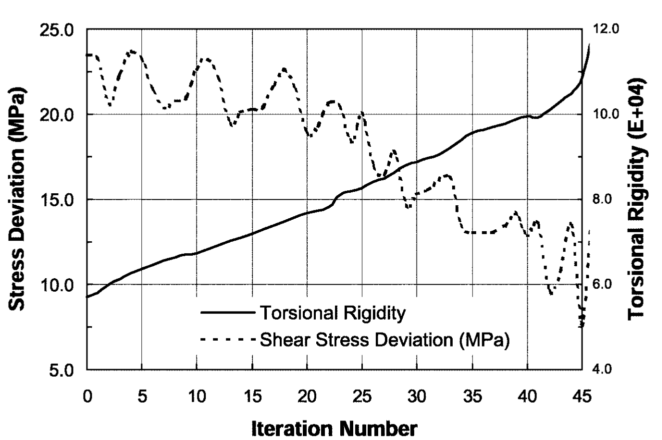

Fig. 9. Evolution histories of shear stress deviation and torsional rigidity

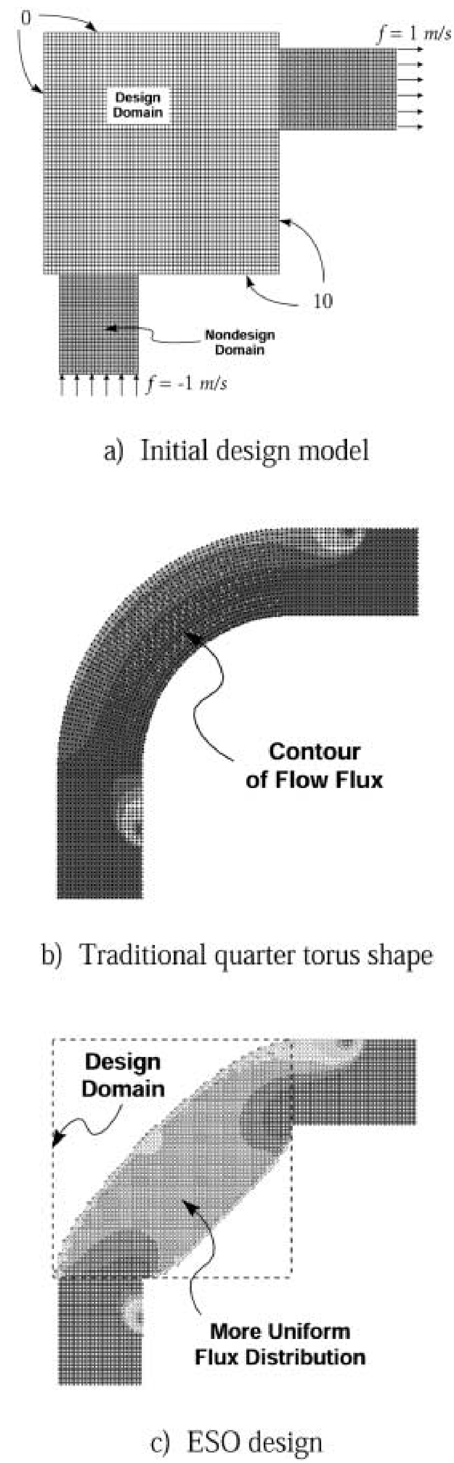

Fig. 10a–c. 90° turn design for inviscid potential flow. **a** Initial design model. **b** Traditional quarter torus shape. **c** ESO design

identified by the rejection ratio are progressively removed, the lowest efficiency level of the material usage gets higher and higher. This can be observed through drawing the contour of flux density as shown in Fig. 10b, c. Compared to the traditional design of a quarter toroid (Fig. 10b), it is found that the ESO solution (Fig. 10c) has a much more uniform flux distribution. This means the ESO design does produce a more even usage of field space.

4.4 Design of electrostatic field

In this example, the shielded profile design for a microstrip transmission line is taken into account as illustrated in Fig. 11a. When the microstrip line operates at low frequency, its capacitance and inductance, thus characteristic impedance, can be obtained from a static analysis (Jin, 1993). The electric potential on the microstrip line is assumed to 1 V while that on the shielding conductor is zero (e.g. it is earthed). To save shielding material and minimize the sheathing space for such designs it is desirable to have as uniform an electric field intensity on the sheath conductor as possible.

The analysis domain is discretized into 80×40 square elements as Fig. 11a. The evolution process starts from a fully populated design domain. As the elements with relative low field intensity are removed, the intensity deviation on the shielded boundary gets smaller and smaller. In other words, the ESO process is one that makes the outer surface iso-field intensity. This can be monitored from the evolution history of the ratio of the highest intensity to the lowest one as Fig. 12. It is found that, after the volume ratio of 50%, the deviation gets almost unchanged, which means the field intensity on the shielding conductor is close to uniform. Figure 11b corresponds to the optimum design at volume ratio $V/V_0 = 50\%$.

4.5 Design of magnetostatic field

This example considers the optimal design of an infinitely long cable with a rectangular stranded inner conductor carrying a forward current of 24 A which is returned through the outside sheath as illustrated in

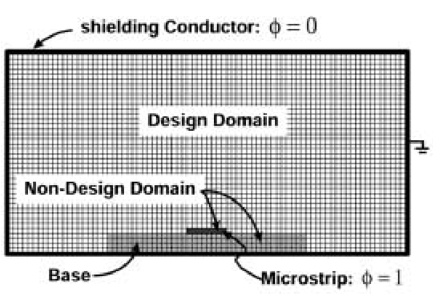

a) Design model of the cross-section

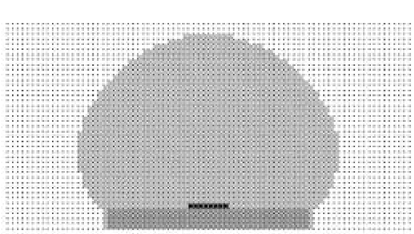

b) Optimized design of the shielded surface (Steady State 20, V/Vo=50%)

Fig. 11a, b. Optimized shielding design of low-frequency microstrip transmission line. **a** Design model of the cross-section. **b** Optimized design of the shielded surface (Steady State 20, $V/V_0 = 50\%$)

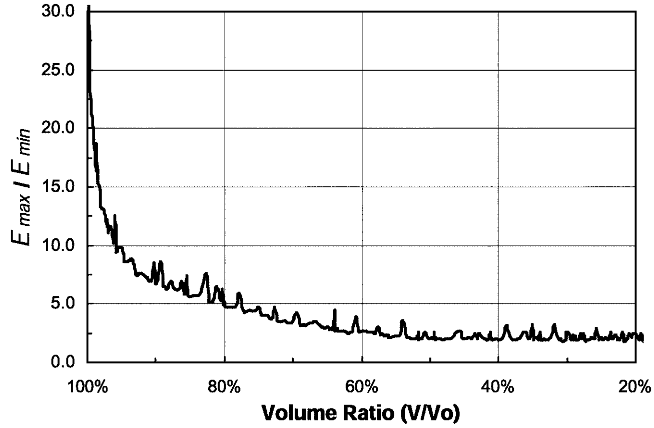

Fig. 12. Uniformized process of boundary electric field intensity

Fig. 13a. In this system, the inner conductor is made of several tightly wound strands of conductor insulated from each other so as to force the currents to flow through the entire cross section of the conductor efficiently. The cross section of each strand is small compared with the depth of penetration so that no skin effect is possible within a strand. Hence the electrical current density in the inner conductor is assumed uniform (Ratnajeevan and Hoole, 1989).

The cable is designed to appropriately re-allocate the sheath conductor and insulation material so as to best

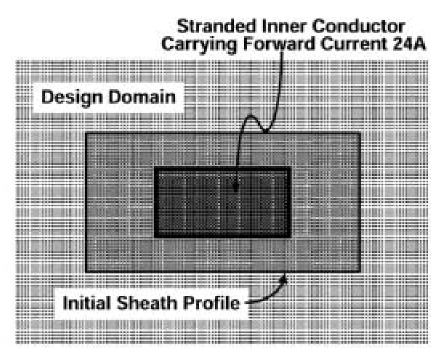

a) Initial design model for cable cross section

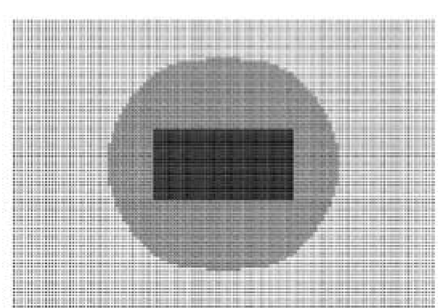

b) Optimized design of magnetic sheath boundary

Fig. 13a, b. Cable sheath profile design with constant volume. **a** Initial design model for cable cross-section. **b** Optimized design of magnetic sheath boundary

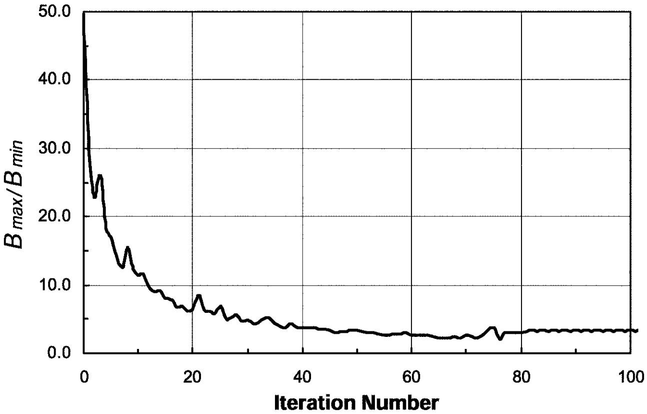

Fig. 14. Evolution history of magnetic flux density on sheath surface

shield the mutual inductance between the inner and the outer conductors. The evolution process starts from a rectangular design as shown in Fig. 13a and then the material is progressively shifted from under utilized area to the over utilized area whilst maintaining a constant cross sectional area. Shown in Fig. 13b is the optimized design, which is close to a circular profile as are most designs of real cables. The uniformity of the magnetic flux density on sheath boundary is shown in Fig. 14, where the ratio of highest flux density to the lowest flux density becomes significantly smaller and smaller as the evolution process progresses.

5
Concluding remarks

A unified evolutionary optimization procedure is proposed to deal with the general steady field problems governed by the quasi-harmonic equation. The relative efficiency of elemental material usage is considered as an optimality criterion to determine the presence and absence of the element. The procedure is presented in an engineering orientated manner, whereby only the standard inputs and outputs of finite element programs are employed. This provides a means for engineers to implement the procedure for various physical field problems on their design platforms without involving too much extra work.

The method presents two procedures for different design purposes. One starts from a design domain with fully populated candidate elements, then gradually removes the under-utilized elements from the analysis model. As a result, the efficiencies of the remaining material become higher than a certain threshold level. Another starts from a feasible initial design, then progressively shifts material from under-utilized area to over-utilized area. Thus, the material allocation becomes more balanced and its usage becomes more efficient.

A number of common design situations with different physical meanings are presented in this paper. These include steady heat conduction, elastic torsion shafts, inviscid incompressible fluid flow, electrostatic field and magnetostatic field. The design examples represent a mixture of existing benchmarks and practical applications, involving shape and topology optimization under single and multiple 'load' cases, using volume reduction and volume constant procedures.

References

Adali S (1981) Cross-sectional shape of an anisotropic, hollow bar with maximum torsional stiffness. Eng. Opt. 5: 169–177

Bendsøe MP (1995) Optimization of Structural Topology, Shape, and Material, Springer-Verlag, Berlin

Haftka RT (1981) Techniques for thermal sensitivity analysis. Int. J. Num. Meth. Eng. 17: 71–80

Hinton E, Owen DRJ (1979) An Introduction to Finite Element Computation, Pineridge Press Limited, Swansea UK

Hinton E, Sienz J (1995) Fully stressed topological design of structure using an evolutionary procedure. Eng. Comput. 12: 229–244

Jin J (1993) The Finite Element Method in Electromagnetics, John Wiley & Sons, New York

Lee BY (1993) Shape sensitivity formulation for an axisymmetric thermal conducting solids. Proceedings of Institution of Mechanical Engineers Part C. J. Mech. Eng. Sci. 207(C3): 209–216

Li Q, Steven GP, Querin OM, Xie YM (1997) Optimal shape design for steady heat conduction by the evolutionary procedure. In: Dulikravich GS, Woodbury KA (eds) Inverse Problems in Heat Transfer and Fluid Flow, vol. 340, pp. 159–164, ASME HTD

Li Q, Steven GP, Querin OM, Xie YM (1999a) Evolutionary optimisation for cross sectional shape of torsional shafts. In: Proceedings of the 3rd World Congress on Multidisciplinary Structural Optimisation, 17–21 May, Buffalo, New York, USA

Li Q, Steven GP, Querin OM, Xie YM (1999b) Shape and topology design for heat conduction by evolutionary structural optimization. Int. J. Heat and Mass Transfer 42: 3361–3371

Li Q, Steven GP, Xie YM (1999c) On equivalence between stress criterion and stiffness criterion in evolutionary structural optimization. Struct. Opt. 18: 67–73

Neittannmaki P, Rudnicki M, Savini A (1996) Inverse Problems and Optimal Design in Electricity and Magnetism, Oxford University Press

Madsen JJ (1995) Shape optimization of internal flow devices via semi-analytical design sensitivities. In: Proceeding of the 1st ISSMO World Congress on Structural and Multidisciplinary Optimization, Goslar, Germany

Mattheck C (1998) Design in Nature, Springer-Verlag, Berlin

Park CW, Yoo YM (1988) Shape design sensitivity analysis of a two-dimensional heat transfer system using the boundary element method. Comp. Struct. 28: 543–550

Polya G (1948) Torsional rigidity, principal frequency, electrostatic capacity and symmetrization. Quar. Appl. Math. 6: 267–277

Polya G, Weinstein A (1950) On the torsional rigidity of multiple connected cross-sections. Ann. Math. 52: 154–163

Querin OM, Steven GP, Xie YM (1998) Evolutionary structural optimisation using a bi-directional algorithm. Eng. Comput. 15: 1031–1048

Ratnajeevan S, Hoole H (1989) Computer-Aided Analysis and Design of Electromagnetic Devices, Elsevier, New York

Rozvany GIN, Bendsøe MP, Kirsch U (1995) Layout optimization of structures. Appl. Mech. Rev. 48: 41–118

Saigal S, Chandra A (1991) Shape sensitivities and optimal configurations for heat diffusion problems: a BEM approach. Trans. ASME: J. Heat Transfer 113: 287–295

Schramm U, Pilkey WD (1993) Structural shape optimization for the torsion problem using direct integration and B-splines. Comp. Meth. Appl. Mech. Eng. 107: 251–268

Seireg AA, Rodriguez J (1997) Optimizing the Shape of Mechanical Elements and Structures, Marcel Dekker Inc., New York

Steven GP, Querin OM, Guan H, Xie YM (1998) Structural Optimisation, Oxbridge Press, Melbourne

Xie YM, Steven GP (1993) A simple evolutionary procedure for structural optimization. Comp. Struct. 49: 885–896

Xie YM, Steven GP (1994) Optimal design of multiple load case structures using an evolutionary procedure. Eng. Comput. 11: 295–302

Xie YM, Steven GP (1997) Evolutionary Structural Optimization, Springer-Verlag, Berlin

Youn SK, Park SH (1997) A study on the shape extraction process in the structural topology optimization using homogenization material. Comp. Struct. 62: 527–538